

## Amorphous Solid Dispersion of $\alpha$ -Mangosteen with PVP K30 Enhances Solubility and Antiproliferative Activity against DU145 Prostate Cancer Cells

Deby Tristiyanti<sup>1,3</sup>, Sriwidodo<sup>2</sup>, Arif Budiman<sup>2</sup>, Syarif Hamdani<sup>3</sup>, Diki Prayugo Wibowo<sup>3</sup>

<sup>1</sup>Doctoral Program of Pharmacy, Faculty of Pharmacy, Padjadjaran University, Sumedang, Indonesia

<sup>2</sup>Department of Pharmaceutical, Faculty of Pharmacy, Universitas Padjadjaran, Sumedang, Indonesia

<sup>3</sup>Sekolah Tinggi Farmasi Indonesia, Bandung, Indonesia

### Correspondence:

Deby Tristiyanti - Email: [deby22002@mail.unpad.ac.id](mailto:deby22002@mail.unpad.ac.id)

### ABSTRACT

Prostate cancer is one of the leading causes of cancer-related death in men worldwide. The natural compound  $\alpha$ -Mangosteen (AM), a xanthone derivative from the fruit rind of *Garcinia mangostana* L., is known to have strong anticancer activity. However, its clinical use is still limited due to its very low water solubility and bioavailability. This study aims to compare the antiproliferative activity of pure AM and amorphous solid dispersion (ASD-AM) against DU145 prostate cancer cells. Amorphous solid dispersions were prepared using the carrier polymer polyvinylpyrrolidone (PVP) K30 via the solvent evaporation method. Physicochemical characterization was performed using Powder X-Ray Diffraction (PXRD), Differential Scanning Calorimetry (DSC), and Fourier-Transform Infrared Spectroscopy (FTIR). Cytotoxicity tests against DU145 prostate cancer cells and normal Vero cells were performed using the MTT method to determine the IC<sub>50</sub> value and selectivity index (SI). The results showed that ASD-AM had an IC<sub>50</sub> value of 22.19  $\mu$ g/mL, which was lower than pure AM (47.34  $\mu$ g/mL), with SI values of 1.99 and 2.15, respectively. The increased antiproliferative activity of ASD-AM is associated with a change in physicochemical properties to an amorphous form, which enhances solubility and dissolution rate.

Overall, the amorphous AM solid dispersion formulation has the potential to enhance its biological effectiveness as a natural anticancer agent for the development of prostate cancer therapy.

**Keywords:**  $\alpha$ -Mangosteen, amorphous solid dispersion, PVP K30, DU145, antiproliferative, prostate cancer.

**How to Cite:** Deby Tristiyanti, Sriwidodo, Arif Budiman, Syarif Hamdani, Diki Prayugo Wibowo, (2025) Amorphous Solid Dispersion of  $\alpha$ -Mangosteen with PVP K30 Enhances Solubility and Antiproliferative Activity against DU145 Prostate Cancer Cells, *Journal of Carcinogenesis*, Vol.24, No.4, 278-285.

### 1. INTRODUCTION

Prostate cancer is one of the most common types of cancer affecting men and is a leading cause of cancer-related deaths worldwide (Filippi & Chiaravalloti, 2023). Conventional therapies such as androgen ablation and chemotherapy often show low effectiveness in advanced stages due to the development of hormone resistance (Berruti & Dalla Volta, 2017). This condition underscores the need for an alternative approach that utilizes natural bioactive compounds with high effectiveness and low toxicity.

One potential candidate is  $\alpha$ -Mangosteen (AM), a xanthone derivative compound isolated from the fruit rind of *Garcinia mangostana* L. Various studies have reported the biological activity of AM, including antioxidant, anti-inflammatory, antibacterial, and anticancer properties (Kalick et al., 2022). AM is known to induce apoptosis in various types of cancer cells, including prostate cancer, thru the activation of caspases and the mitochondrial pathway (Majdalawieh et al., 2024; Dewi et al., 2024).

The main obstacle to the clinical use of AM is its very low water solubility, which is only about 2  $\mu$ g/mL, resulting in limited bioavailability (Budiman et al., 2022). One promising approach to address this is the formation of amorphous solid dispersions (ASDs) using hydrophilic polymers such as PVP K30, which can improve solubility, dissolution rate, and

physical stability (Dindigala et al., 2024; Qayyum et al., 2022).

This study aims to compare the antiproliferative activity between pure AM and amorphous solid dispersion form of  $\alpha$ -Mangosteen (ASD-AM) against DU145 prostate cancer cells, and to analyze the relationship between changes in physicochemical properties and the resulting increase in biological activity.

## 2. MATERIALS AND METHODS

### Materials

$\alpha$ -Mangosteen ( $\geq 98\%$ ) was obtained from Chengdu Biopurify Phytochemicals (Shincuan, China), while the PVP K30 polymer was obtained from Merck (Germany). Phosphate buffer, DMSO, MTT, and trypsin-EDTA were obtained from Gibco (Thermo Fisher, USA). Prostate cancer cells DU145 and normal cells Vero were obtained from LIPI, Indonesia. All chemicals used have an analytical purity level.

### Preparation of Amorphous Solid Dispersions (ASDs).

ASD-AM was prepared by the solvent evaporation method. AM and PVP K30 were dissolved in methanol with drug-to-polymer weight ratios of 1:1, 1:3, and 1:5, respectively. The solution mixture was then evaporated using a rotary evaporator (Buchi Rotavapor-R) connected to a water bath (BM200, Yamato Scientific, Santa Clara, CA, USA) at 30 °C until the solvent was completely evaporated. The resulting residue was dried at 30 °C for 72 hours in an oven until dry ASD-AM powder was obtained.

### Physicochemical Characterization

#### *Powder X-Ray Diffraction (PXRD)*

X-ray diffraction patterns were collected using a Bruker D8 Advance diffractometer (Siemens, Berlin, Germany) with operating conditions of 40 kV and 40 mA, a Cu target with Ni filter, a scan rate of 1°/minute, and a  $2\theta$  range between 10–40°. The halo pattern without sharp diffraction peaks indicates the formation of an amorphous phase.

#### *Differential Scanning Calorimetry (DSC)*

DSC measurements were performed using a Shimadzu DSC-60 Plus (Kyoto, Japan). The sample (3–5 mg) was sealed in an aluminum container and heated from 0 to 280 °C at a heating rate of 10 °C/min under a nitrogen flow of 20 mL/min.

#### *Fourier-Transform Infrared Spectroscopy (FTIR)*

FTIR spectra were obtained using a Shimadzu Prestige-21 (Kyoto, Japan). Each sample (1–2 mg) was mixed with 200–250 mg of KBr, ground, and compressed into a pellet at a pressure of 60 psi. The spectrum was recorded in the wavenumber range of 4000–400  $\text{cm}^{-1}$  to observe the functional group interactions between AM and PVP K30.

### Solubility Test

The crystalline and amorphous solubility of AM was determined in 50 mM phosphate buffer (pH 7.4) at 37 °C. An excess amount of sample was shaken for 48 hours, then filtered thru a 0.45  $\mu\text{m}$  membrane and analyzed using HPLC after dilution with the mobile phase.

### HPLC Analysis

Liquid chromatography analysis was performed using an Agilent HPLC system (Hewlett-Packard Strasse 8, Waldbronn, Germany). Separation was performed on an Eclipse Plus C18 column (4.6  $\times$  150 mm, 5  $\mu\text{m}$ ) with a column temperature of 30 °C. The mobile phase consisted of a mixture of methanol:water (95:5, v/v), and detection was carried out at a wavelength of 254 nm. The concentration range of the standard solutions is between 4–128  $\mu\text{g/mL}$ .

### Entrapment Efficiency (EE%)

Entrapment efficiency is determined by dissolving each ASD-AM sample in methanol to obtain an AM concentration of 100  $\mu\text{g/mL}$ . The solution was stirred for 30 minutes, filtered using a 0.45  $\mu\text{m}$  membrane, diluted with acetonitrile, and analyzed by HPLC.

Calculation formula:

$$EE(\%) = \frac{\text{Measured concentration}}{\text{Theoretical concentration}} \times 100$$

### In Vitro Dissolution Test

The dissolution test was performed using the paddle method. ASD powder containing an equivalent amount of 40  $\mu\text{g/mL}$  AM was dispersed in 500 mL of phosphate buffer (pH 7.4) at 37 °C and stirred at a speed of 150 rpm. Samples (5 mL)

were taken at specific time points (1–150 minutes), filtered (0.45  $\mu$ m), diluted with acetonitrile, and analyzed by HPLC.

### Storage Stability Test

The physical stability of ASD was tested for 30 days under two storage conditions: (a) 25 °C/0% RH in a desiccator with silica gel, and (b) 25 °C/90% RH in a desiccator with saturated potassium nitrate. Changes in crystallinity after storage were evaluated using PXRD.

### Cancer Cell Inhibition Assay (MTT Assay)

The cytotoxic activity of AM and ASD-AM was evaluated using the MTT assay method against DU145 cells (prostate cancer) and Vero cells (normal cells). Cells ( $3 \times 10^4$ /well) were cultured in a 24-well plate and incubated for 24 hours at 37 °C with an atmosphere of 5% CO<sub>2</sub>. The medium was replaced with fresh medium containing AM or ASD-AM at various concentrations. After 48 hours of incubation, MTT (0.5 mg/mL) was added and incubated for 4 hours. The formazan crystals formed were dissolved in 1000  $\mu$ L of DMSO, and then the absorbance was read at a wavelength of 595 nm using an ELISA reader. Cell viability was calculated as a percentage of the control, and the IC<sub>50</sub> value was determined from the concentration-response curve.

## 3. RESULTS

### Physicochemical Characterization

Analysis using PXRD showed that pure AM has sharp and well-defined diffraction peaks, indicating a crystalline form with high structural order. In contrast, the amorphous solid dispersion of  $\alpha$ -Mangosteen–PVP K30 exhibited a halo pattern without sharp peaks at all ratios, indicating that AM had transformed into an amorphous form. This phase change is important because the amorphous form has higher free energy and can potentially improve solubility and bioavailability (Bhujbal et al., 2021).

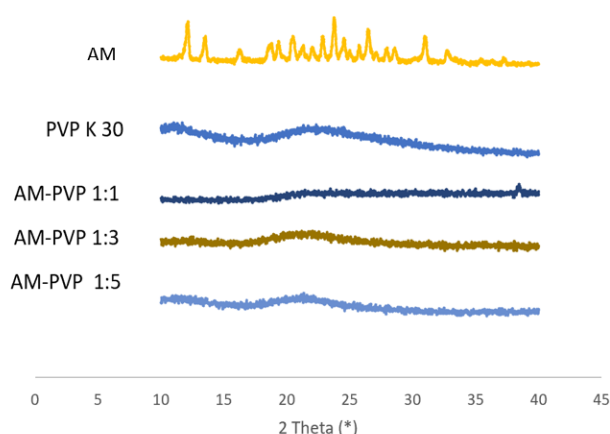


**Figure 1. Diffractogram of AM and ASD AM-PVP K30**

DSC analysis shows that pure AM has a sharp endothermic peak at around 177 °C, representing the typical melting point of the crystalline form. In ASD AM–PVP K30, this endothermic peak no longer appears; only a baseline shift indicating the glass transition (T<sub>g</sub>) is visible. These results suggest that AM loses its crystalline structure and transforms into an amorphous phase due to intermolecular interactions between AM and PVP K30 (Budiman et al., 2023).

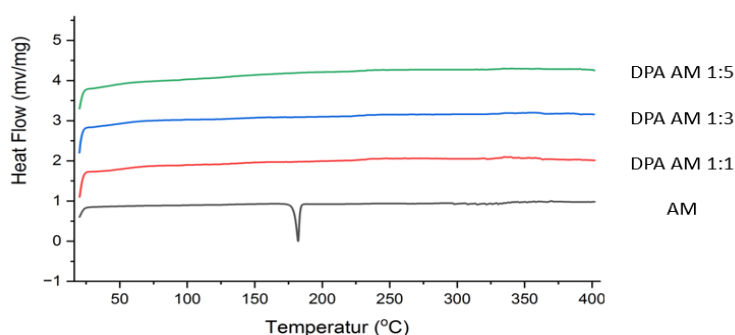


**Figure 2. Thermograms of AM and ASD AM-PVP K30**

The FTIR spectrum shows significant wavenumber shifts, especially in the carbonyl (C=O) and hydroxyl (O–H) bands, indicating the presence of hydrogen bonds between AM and PVP K30. The shift of the carbonyl group from  $1644\text{ cm}^{-1}$  to approximately  $1676\text{ cm}^{-1}$  and the hydroxyl group from  $3420\text{ cm}^{-1}$  to  $3480\text{ cm}^{-1}$  supports the occurrence of this interaction (Wu et al., 2023).

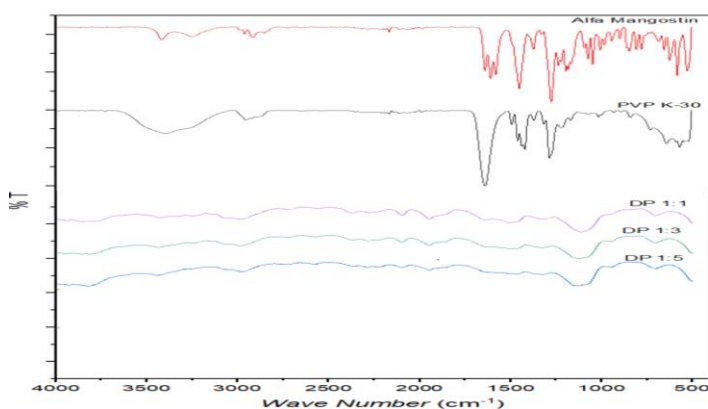


**Figure 3. FTIR Spectra of AM and ASD AM-PVP K30**

### Entrapment Efficiency (EE%)

The entrapment efficiency (EE%) values are in the high range, above 80%.

**Table 1. Entrapment Efficiency/EE (%) AM and ASD AM-PVP K30**

Sample	EE (%)
ASD $\alpha$ Mangosteen-PVP 1:1	$84.24 \pm 0.06$
ASD $\alpha$ Mangosteen-PVP 1:3	$87.50 \pm 0.62$
ASD $\alpha$ Mangosteen-PVP 1:5	$88.74 \pm 0.53$

The ASD formulations of  $\alpha$ -Mangosteen–PVP K30 at ratios of 1:1, 1:3, and 1:5 showed EE values of  $84.24 \pm 0.06\%$ ,  $87.50 \pm 0.62\%$ , and  $88.74 \pm 0.53\%$ , respectively. These results indicate that most of the AM molecules were successfully entrapped within the polymer matrix, signifying that the ASD manufacturing process via the solvent evaporation method was effective with strong interactions between the drug and the polymer (Rusdin et al., 2024).

### Solubility and Dissolution

The solubility of pure AM is only  $2.04 \pm 0.009\text{ }\mu\text{g/mL}$ , while ASD AM–PVP K30 (1:3 ratio) reaches  $64.58 \pm 1.08\text{ }\mu\text{g/mL}$ , an increase of approximately 30 times. Dissolution testing showed that over 85% of AM was released from ASD within the first 20 minutes, compared to less than 10% from the pure form after 60 minutes. This increase is due to the interaction of hydrogen bonds with PVP K30, which improves wettability and stabilizes supersaturated conditions (Tekade et al., 2020).

**Table 2. Solubility of AM and ASD in AM-PVP K30**

Sample	Concentration ( $\mu\text{g/mL}$ )	Solubility Increase
$\alpha$ Mangosteen	$2.04 \pm 0.009$	
ASD $\alpha$ Mangosteen-PVP K30 1:1	$17.70 \pm 0.7269$	10
ASD $\alpha$ Mangosteen-PVP K30 1:3	$64.58 \pm 1.0783$	30
ASD $\alpha$ Mangosteen-PVP K30 1:5	$61.06 \pm 0.0598$	30

The solubility test results showed that pure AM has very low solubility, only  $2.04 \pm 0.009\text{ }\mu\text{g/mL}$ , confirming its nature as a hydrophobic compound with limited water solubility. After being formulated into an amorphous solid dispersion (ASD) system with PVP K30 polymer, solubility significantly increased.

At a ratio of 1:1, the solubility of AM reached  $17.70 \pm 0.7269\text{ }\mu\text{g/mL}$ , or approximately a 10-fold increase compared to its pure form. A greater increase was observed at ratios of 1:3 and 1:5, with solubilities of  $64.58 \pm 1.0783\text{ }\mu\text{g/mL}$  and  $61.06 \pm 0.0598\text{ }\mu\text{g/mL}$ , respectively, indicating an approximately 30-fold increase compared to pure  $\alpha$ -Mangosteen.

This increase in solubility indicates strong intermolecular interactions between AM and PVP K30 thru hydrogen bonds, which play a role in increasing wettability and forming stable supersaturated conditions during the dissolution process.

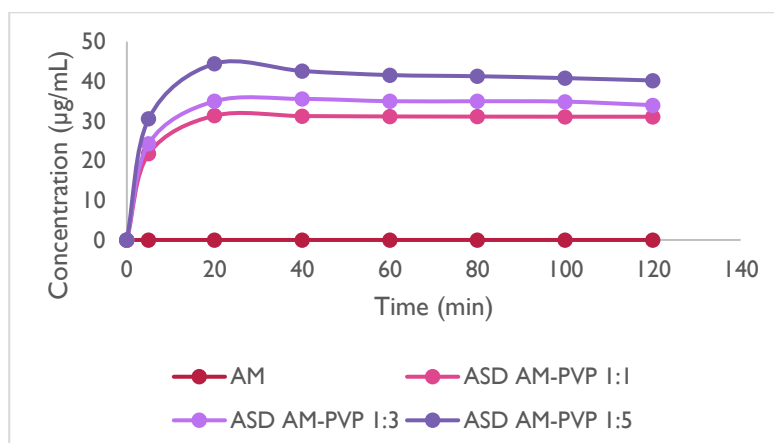


**Figure 4. Dissolution Rate of AM and ASD AM–PVP K30**

The dissolution rate profile shows that pure AM is only slightly soluble and dissolves very slowly. Conversely, the entire ASD formulation showed a significant increase in drug release rate. The 1:5 ratio formulation showed the highest release, reaching a concentration of approximately 60–70  $\mu\text{g/mL}$  in the first 20 minutes, indicating improved dissolution efficiency due to the structural change to an amorphous form.

#### Stability at 0% RH and 90% RH

This stability test aims to evaluate whether the amorphous form of the solid dispersion system can maintain its stability during storage or undergoes recrystallization. Under low humidity conditions (RH 0%), all ASD AM–PVP K30 (1:5) samples showed a halo diffraction pattern without sharp crystalline peaks up to day 30, indicating that the amorphous AM structure remained stable during dry storage. The polymer PVP K30 plays an important role in maintaining this stability by forming hydrogen bonds with  $\alpha$ -Mangosteen, which limits the mobility of drug molecules and inhibits the formation of new crystal nuclei (Husan et al., 2025; Rusdin et al., 2024).

Conversely, under high humidity conditions (RH 90%), small changes in the diffraction pattern began to appear, particularly at ratios of 1:1 and 1:3, where low-intensity crystal peaks emerged after 7 to 30 days of storage. This phenomenon indicates partial recrystallization due to water vapor absorption by PVP K30, which increases molecular mobility and reduces the stability of the amorphous phase.

The 1:5 ratio formulation still showed a consistent halo pattern up to day 30, indicating higher moisture stability. Increasing the amount of polymer was proven to strengthen the intermolecular interactions between PVP K30 and  $\alpha$ -Mangosteen, and to form a dense solid matrix, thereby slowing down water vapor diffusion and preventing recrystallization. Based on these results, the ASD AM–PVP K30 (1:5) formulation was selected as the most stable system and used for further antiproliferative activity testing.

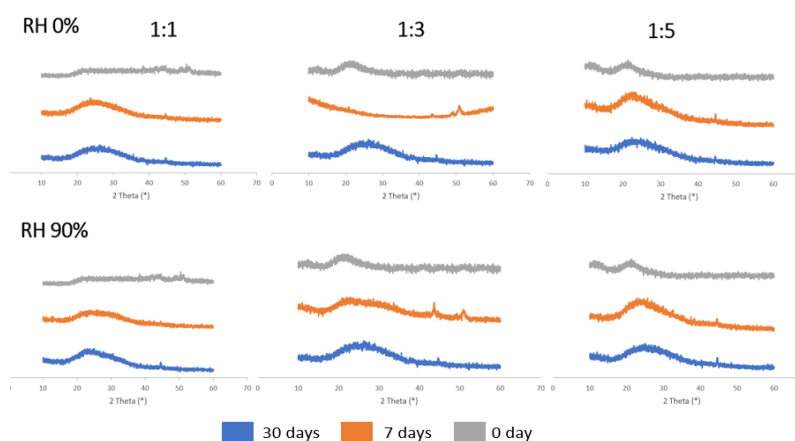


**Figure 5 Stability of AM and ASD AM–PVP K30 at 0% and 90% RH**

### Antiproliferative Activity

The MTT assay showed that both pure AM and ASD AM–PVP K30 (1:5) have the ability to inhibit the growth of DU145 prostate cancer cells in a dose-dependent manner. The IC<sub>50</sub> value for pure AM was 47.34  $\mu$ g/mL, while ASD AM–PVP K30 showed a lower value of 22.19  $\mu$ g/mL, indicating an increase in cytotoxic potential against cancer cells.

**Table 3. Results of antiproliferative activity tests (IC 50) of AM and ASD AM-PVP K30 on DU 145 prostate cancer cells and normal Vero cells**

Sampel	Prostate Cancer Cells (DU 145)	R'	Normal Cell (Vero)	R'	SI
	IC 50 ( $\mu$ g/mL)		IC 50 ( $\mu$ g/mL)		
$\alpha$ Mangosteen	47,3415	0,9894	101,5714	0,9894	2,15
ASD $\alpha$ Mangosteen- PVP K30	22,1867	0,9515	44,2367	0,9700	1,99

The IC<sub>50</sub> values against standard Vero cells were 101.57  $\mu$ g/mL for pure AM and 44.24  $\mu$ g/mL combination ASD AM–PVP K30. The ASD formulation exhibited a minor reduction in the selectivity index (SI) from 2.15 to 1.99; however, its enhanced antiproliferative efficacy indicates higher bioavailability and cellular penetration resulting from the transition from crystalline to amorphous form.

The conversion of AM into an amorphous state enhances its solubility and dissolution rate, hence increasing the quantity of drug molecules that can interact with cancer cell membranes. This behavior corresponds with the hypothesis that amorphous forms possess elevated free energy and vapor pressure relative to crystalline forms, hence amplifying their biological effects (Schittny et al., 2019).

The results demonstrate that the amorphization of AM within the PVP K30 matrix markedly improves its antiproliferative efficacy, while maintaining a selective toxicity towards cancer cells over normal cells. The ASD AM–PVP K30 (1:5) formulation, exhibiting an ideal equilibrium of efficacy and selectivity, was identified as the most promising contender for the advancement of natural product-derived anticancer therapy.

## 4. DISCUSSION

This study illustrates that converting AM into an amorphous solid dispersion (ASD) with PVP K30 significantly improves its solubility, dissolution rate, and antiproliferative efficacy against DU145 prostate cancer cells. The carrier polymer PVP K30 effectively stabilises the amorphous form by forming hydrogen bonds with the hydroxyl and carbonyl groups of AM, thereby inhibiting recrystallisation and preserving a supersaturated state during dissolution (Saluja et al., 2016 ; Rusdin et al., 2024). PXRD and DSC investigations validated the amorphous transformation, whilst FTIR spectra corroborated the chemical interactions that enhance stability and dissolving efficacy (Kulawik et al., 2025).

The solubility enhancement from 2.04  $\mu$ g/mL in crystalline form to over 60  $\mu$ g/mL in the ASD significantly elevated the concentration of the drug available for cellular absorption, hence amplifying cytotoxicity. This outcome corresponds with the idea that amorphous materials, having elevated free energy, facilitate increased molecule dispersion and solvation (Budiman et al., 2023). The decrease of IC<sub>50</sub> from 47.34  $\mu$ g/mL (pure AM) to 22.19  $\mu$ g/mL (ASD AM PVP K30 1:5) substantiates the direct correlation between enhanced solubility and biological efficacy. A minor reduction in the selectivity index (SI) was noted; nevertheless, the values continue to fall within the permitted limits for natural anticancer drugs, suggesting that enhanced solubility slightly increased exposure to normal cells without undermining selectivity (Rusdin et al., 2024).

The enhanced antiproliferative action can be ascribed to the increased water solubility of AM and possibly augmented membrane permeability due to PVP K30. Increased intracellular levels may potentiate apoptotic signalling pathways associated with AM, including mitochondrial ROS production and caspase activation (Zafar et al., 2018). Subsequent studies examining apoptosis or caspase tests would be beneficial to validate these cellular pathways and enhance the relationship between physicochemical and biological results (Bhat et al., 2025).

Stability experiments indicated that the amorphous form maintained stability for 30 days in dry conditions but partially recrystallised at elevated humidity (90% RH), especially in formulations with reduced polymer ratios. The 1:5 ratio preserved amorphous stability more efficiently, indicating that sufficient polymer encapsulation restricts molecular mobility and moisture-driven nucleation. This discovery underscores the essential function of polymer content in maintaining physicochemical stability and dissolving efficacy during storage (Tizaoui et al., 2025).



The elevated entrapment efficiency (>84%) in all formulations indicates superior compatibility between AM and PVP K30, validating the efficacy of the solvent evaporation technique in integrating the medication into the polymer matrix (Bhalodiya et al., 2021). The dissolution profiles indicated a polymer ratio-dependent impact, with increased PVP K30 concentrations resulting in accelerated and more comprehensive drug release. This observation corresponds with the "spring and parachute" paradigm, wherein the amorphous state facilitates fast supersaturation (spring), while the polymer stabilises it (parachute) by inhibiting nucleation (Bhalodiya et al., 2021).

These findings collectively demonstrate that the AM–PVP K30 ASD successfully surmounts the compound's intrinsic solubility limitations, resulting in improved biological efficacy. The optimisation of the drug-to-polymer ratio enhanced solubility and dissolution while augmenting cytotoxic potency, thereby demonstrating a definitive structure–performance relationship. This formulation establishes a robust basis for subsequent pharmacokinetic and bioavailability investigations in animal models, essential for validating the in vivo therapeutic efficacy of the system (AL-Japairai et al., 2020).

This study emphasises a wider significance for poorly soluble natural compounds, in addition to AM. The effective implementation of ASD technology illustrates how logical formulation strategies can connect phytochemical research with pharmaceutical development. The integration of natural product pharmacology with contemporary solid dispersion techniques is a viable strategy to improve the therapeutic potential of hydrophobic xanthenes and polyphenols facing analogous solubility issues (Rusdin et al., 2024).

## 5. CONCLUSION

The transformation of AM into an amorphous solid dispersion (ASD) form using PVP K30 successfully significantly improved solubility and dissolution rate. These changes directly contribute to increased antiproliferative activity against DU145 prostate cancer cells. Although there was a slight decrease in selectivity toward normal cells, ASD AM–PVP K30 shows great potential for development as a natural product-based chemotherapy candidate. Further in vivo studies and the development of targeted formulations are recommended to support its clinical application.

## 6. ACKNOWLEDGEMENT

The cost to publish this article was covered by Universitas Padjadjaran through the Indonesian Endowment Fund for Education (LPDP), which is part of the Indonesian Ministry of Higher Education, Science and Technology, and is managed under the EQUITY Program (Contract Nos. 4303/B3/DT.03.08/2025 and 3927/UN6.RKT/HK.07.00/2025), along with the Indonesian Education Scholarship

## REFERENCES

- [1] AL-Japairai, K. A. S., AL-Japairai, K. A. S., Alkhalidi, H. M., Mahmood, S., Almurisi, S. H., Doolaanea, A. A., Al-Sindi, T. A., Chatterjee, B., & Chatterjee, B. (2020). *Lyophilized Amorphous Dispersion of Telmisartan in a Combined Carrier–Alkalizer System: Formulation Development and In Vivo Study*. 5(50), 32466–32480. <https://doi.org/10.1021/ACSOMEGA.0C04588>
- [2] Bhat, I. A., Bhat, A. M., & Abdullah, S. T. (2025). *Apoptosis-Mechanisms, Regulation in Pathology, and Therapeutic Potential*. <https://doi.org/10.5772/intechopen.1008890>
- [3] Berruti, A., & Dalla Volta, A. (2017). *Resistance to hormonal therapy in prostate cancer* (Vol. 249, pp. 181–194). Springer, Cham. [https://doi.org/10.1007/164\\_2017\\_21](https://doi.org/10.1007/164_2017_21)
- [4] Bhujbal, S. V., Mitra, B., Jain, U., Gong, Y., Agrawal, A., Karki, S., Taylor, L. S., Kumar, S., & Zhou, Q. (2021). Pharmaceutical amorphous solid dispersion: A review of manufacturing strategies. *Acta Pharmaceutica Sinica B*, 11(8), 2505–2536. <https://doi.org/10.1016/j.apsb.2021.05.014>
- [5] Budiman, A., Citraloka, Z. G., Muchtaridi, M., Sriwidodo, S., Aulifa, D. L., & Rusdin, A. (2022). Inhibition of crystal nucleation and growth in aqueous drug solutions: Impact of different polymers on the supersaturation profiles of amorphous drugs—The case of alpha-Mangosteen. *Pharmaceutics*, 14(11), 2386. <https://doi.org/10.3390/pharmaceutics14112386>
- [6] Budiman, A., Handini, A. L., Muslimah, M. N., Nurani, N. V., Laelasari, E., Kurniawansyah, I. S., & Aulifa, D. L. (2023). Amorphous solid dispersion as drug delivery vehicles in cancer. *Polymers*, 15(16), 3380. <https://doi.org/10.3390/polym15163380>
- [7] Dewi, R. C., Alaydrus, S., & Wahyuhandayani, T. (2024). Prostate anticancer activity testing  $\alpha$ -Mangosteen in vitro on DU145 cells using WST-8 method. *Jurnal Penelitian Pendidikan IPA (JPPIPA)*, 10(8), 5851–5855. <https://doi.org/10.29303/jppipa.v10i8.8517>
- [8] Dindigala, A. K., Anitha, P., Makineni, A., & Viswanath, V. S. (2024). A review on amorphous solid dispersions for improving physical stability and dissolution: Role of polymers. *GSC Advanced Research and Reviews*, 19(3), 296–302. <https://doi.org/10.30574/gscarr.2024.19.3.0231>

- [9] Filippi, L., & Chiaravalloti, A. (2023). Prostate cancer: From molecular imaging to immunological and target therapies. *Biomedicines*, 11(4), 1176. <https://doi.org/10.3390/biomedicines11041176>
- [10] Hussan, S., Babu, T. D., & Thayyil, M. S. (2025). Physicochemical characterization and biological evaluation of amorphous solid dispersions of an anticancerous drug: Erlotinib HCl. *Scientific Reports*, 15, 23787. <https://doi.org/10.1038/s41598-025-07692-1>
- [11] Jingya, W., & Van den Mooter, G. (2023). The influence of hydrogen bonding between different crystallization tendency drugs and PVPVA on the stability of amorphous solid dispersions. *International Journal of Pharmaceutics*, 646, 123440. <https://doi.org/10.1016/j.ijpharm.2023.123440>
- [12] Kalick, L. S., Khan, H. A., Maung, E., Baez, Y., Atkinson, A. N., Wallace, C. E., Day, F., Delgadillo, B. E., Mondal, A., Watanapokasin, R., Barbalho, S. M., & Bishayee, A. (2022). Mangosteen for malignancy prevention and intervention: Current evidence, molecular mechanisms, and future perspectives. *Pharmacological Research*, 188, 106630. <https://doi.org/10.1016/j.phrs.2022.106630>
- [13] Kulawik, A., Kulawik, M., Rosiak, N., Lu, W., Cielecka-Piontek, J., & Zalewski, P. (2025). Amorphous Lycopene–PVP K30 Dispersions Prepared by Ball Milling: Improved Solubility and Antioxidant Activity. *Polymers*, 17(21), 2916. <https://doi.org/10.3390/polym17212916>
- [14] Majdalawieh, A. F., Terro, T. M., Ahari, S. H., & Abu-Yousef, I. A. (2024).  $\alpha$ -Mangosteen: A xanthone derivative in mangosteen with potent anti-cancer properties. *Biomolecules*, 14(11), 1382. <https://doi.org/10.3390/biom14111382>
- [15] Mori, D., Dudhat, K., Soniwala, M., Dudhrejiya, A., Shah, S., & Prajapati, B. (2023). A review on stabilization mechanism of amorphous form-based drug delivery system. *Materials Today Communications*, 37, 107411. <https://doi.org/10.1016/j.mtcomm.2023.107411>
- [16] Monika Bhalodiya, Jayant Chavda, Dhaval Mori, Nilesh Patel, Ravi Manek, Kiran Dudhat, (2021), Formulation and evaluation of amorphous solid dispersion Boerhaavia diffusa methanolic root extract for improving dissolution properties, *Journal of Drug Delivery Science and Technology*, Volume 66, 102740, ISSN 1773-2247, <https://doi.org/10.1016/j.jddst.2021.102740>.
- [17] Pandi, P., Bulusu, R., Kommineni, N., Khan, W., & Singh, M. (2020). Amorphous solid dispersions: An update for preparation, characterization, mechanism on bioavailability, stability, regulatory considerations, and marketed products. *International Journal of Pharmaceutics*, 586, 119560. <https://doi.org/10.1016/j.ijpharm.2020.119560>
- [18] Qayyum, M., Ishtiaq, A., Asghar, S., Khan, I. U., Iqbal, M. S., & Khalid, S. H. (2022). Development of the amorphous solid dispersion of curcumin: A rational selection of polymers for enhanced solubility and dissolution. *Crystals*, 12(11), 1606. <https://doi.org/10.3390/cryst12111606>
- [19] Rusdin, A., Mohd Gazzali, A., Thomas, N. A., Megantara, S., Aulifa, D. L., Budiman, A., & Muchtaridi, M. (2024). Advancing drug delivery paradigms: Polyvinylpyrrolidone (PVP)-based amorphous solid dispersion for enhanced physicochemical properties and therapeutic efficacy. *Polymers*, 16(2), 286. <https://doi.org/10.3390/polym16020286>
- [20] Schittny, A., Huwyler, J., & Puchkov, M. (2019). Mechanisms of increased bioavailability through amorphous solid dispersions: A review. *Drug Delivery*, 27(1), 110–127. <https://doi.org/10.1080/10717544.2019.1704940>
- [21] Saluja, H., Mehanna, A., Panicucci, R., & Atef, E. (2016). Hydrogen Bonding: Between Strengthening the Crystal Packing and Improving Solubility of Three Haloperidol Derivatives. *Molecules*, 21(6), 719. <https://doi.org/10.3390/molecules21060719>
- [22] Tekade, A. R., & Yadav, J. N. (2020). A review on solid dispersion and carriers used therein for solubility enhancement of poorly water-soluble drugs. *Advanced Pharmaceutical Bulletin*, 10(3), 359–369. <https://doi.org/10.34172/apb.2020.044>
- [23] Tizaoui, C., Rietveld, I. B., Galai, H., Coquerel, G., Morin-Grognet, S., & Gbabode, G. (2025). “Stabilization” of Amorphous Ketoprofen in Thin Films. *Langmuir*, 41(1), 671–683. <https://doi.org/10.1021/acs.langmuir.4c03933>
- [24] Zafar, A., Pilkington, L. I., Haverkate, N. A., van Rensburg, M., Leung, E., Kumara, S., Denny, W. A., Barker, D., Alsuraifi, A., Hoskins, C., & Reynisson, J. (2018). Investigation into Improving the Aqueous Solubility of the Thieno[2,3-b]pyridine Anti-Proliferative Agents. *Molecules*, 23(1), 145. <https://doi.org/10.3390/MOLECULES23010145>